APS physics

CHORUS

This is the accepted manuscript made available via CHORUS. The article has been published as:

Entrance channel effects on the quasifission reaction channel in Cr + W systems

K. Hammerton, D. J. Morrissey, Z. Kohley, D. J. Hinde, M. Dasgupta, A. Wakhle, E. Williams, I. P. Carter, K. J. Cook, J. Greene, D. Y. Jeung, D. H. Luong, S. D. McNeil, C. Palshetkar, D. C. Rafferty, C. Simenel, and K. Stiefel

Phys. Rev. C **99**, 054621 — Published 23 May 2019

DOI: 10.1103/PhysRevC.99.054621

Entrance Channel Effects on the Quasifission Reaction Channel in Cr + W Systems

K. Hammerton,[1,2,*] D. J. Morrissey,[1,2] Z. Kohley,[1,2] D. J. Hinde,[3] M. Dasgupta,[3] A. Wakhle,[1,3,†] E. Williams,[3] I. P. Carter,[3,‡] K. J. Cook,[3,§] J. Greene,[4] D. Y. Jeung,[3] D. H. Luong,[3,¶] S. D. McNeil,[3] C. Palshetkar,[3,**] D. C. Rafferty,[3] C. Simenel,[3] and K. Stiefel[1,2,††]

[1]*National Superconducting Cyclotron Laboratory, Michigan State University, East Lansing, Michigan 48824, USA*
[2]*Department of Chemistry, Michigan State University, East Lansing, Michigan 48824, USA*
[3]*Department of Nuclear Physics, Research School of Physics and Engineering, Australian National University, Canberra, Australian Capital Territory 2601, Australia*
[4]*Physics Division, Argonne National Laboratory, Lemont, Illinois 60473, USA*

(Dated: March 27, 2019)

Background: Formation of a fully equilibrated compound nucleus is a critical step in the heavy-ion fusion reaction mechanism but can be hindered by orders of magnitude by quasifission, a process in which the dinuclear system breaks apart prior to full equilibration. To provide a complete description of heavy-ion fusion it is important to characterize the quasifission process. In particular, the impact of changing the neutron-richness on the quasifission process is not well known. A previous study of Cr + W reactions at a constant 13 % above the Coulomb barrier concluded that an increase in neutron-richness leads to a decrease in the prominence of the quasifission reaction channel.
Purpose: The dynamics of quasifission for reactions with varying neutron-richness was explored at a constant excitation energy, closer to the interaction barrier than the previous work, to see if the correlation between neutron-richness and quasifission is valid at lower energies.
Methods: Mass distributions were measured at the Australian National University for eight different combinations of Cr + W reactions, using the kinematic coincidence method. To eliminate the effect of differing excitation energies, measurements were made at beam energies chosen to give 52 MeV of excitation energy in all the compound nucleui.
Results: A curvature parameter, describing the shape of the mass distributions, was determined for the fission-like fragment mass distributions for each reaction, and compared to various reaction parameters known to influence quasifission.
Conclusions: The present work demonstrates that at energies near the interaction barrier, the beam energy with respect to the barrier is as important as neutron-richness effects in determining the quasifission characteristics in these Cr + W reactions involving statically deformed target nuclei, and both are important considerations for future heavy and superheavy element production reactions.

PACS numbers: 25.70.Jj, 25.70.Gh, 25.70.-z

I. INTRODUCTION

The fusion of two large nuclei has thus far been the primary mechanism for the formation of superheavy nuclei [1–5]. There is great interest in producing new superheavy nuclei because each additional nucleon furthers our understanding of the limits of nuclear stability [5–7] and there are predictions that there will be a spherical shell closure near N = 184 and Z ≈ 114-126 [8]. Experimental work has already shown indications of a region of enhanced stability in neutron-rich nuclei near Z ≥ 110 and N ≈ 171 - 174 [5, 9]. However, even these very neutron-rich nuclei are still ∼ 10 neutrons away from N=184. To reach nuclei in the N = 184 region more neutron-rich projectiles and targets than the commonly used stable ^{48}Ca and actinide targets will be necessary [2, 5, 8, 10, 11]. The next generation rare isotope facilities will allow exploration of the heavy-ion fusion mechanism with medium-mass, neutron-rich projectiles that can form neutron-rich, lower-mass superheavy nuclei [13–15, 30]. Therefore, it is vital to have an understanding of the effect of increasing the neutron-richness of the system on the heavy-ion fusion reaction mechanism.

The cross section for the formation of a superheavy evaporation residue σ_{evr} has been written as

$$\sigma_{evr} = \sum_{\mathrm{J=0}}^{\mathrm{J_{max}}} \sigma_{\mathrm{cap}}(\mathrm{J})\mathrm{P_{CN}}(\mathrm{J})\mathrm{W_{sur}}(\mathrm{J}), \qquad (1)$$

where J is the angular momentum, σ_{cap} is the capture cross section for a given entrance channel, $\mathrm{P_{CN}}$ is the

* kalee.hammerton@gmail.com; Present address: Savannah River National Laboratory, Aiken, SC 29803, USA
† Present address: Cyclotron Institute, Texas A&M University, College Station, Texas 77843, USA
‡ Present address: CSIRO Sorting and Sensing, Mineral Resources, Building 67, ANSTO, Lucas Heights, Australia.
§ Present address: Tokyo Institute of Technology, Meguro, Tokyo 152-8550, Japan.
¶ Present address: Scandinavian Health Limited, Taiwan Branch, 136 Guosheng 2nd Street, Taoyuan District, Taoyuan City, Taiwan 330.
** Present Address: Tata Institute of Fundamental Research, Mumbai 400005, India
†† Present address: Oak Ridge National Laboratory, Oak Ridge, TN 37831, USA

probability of forming a (compact) compound nucleus, and W_{sur} is the probability of the compound nucleus surviving against fission ([16] and references therein). Following capture, formation of a fully fused compound nucleus can be hindered by the early separation of the dinuclear system, termed quasifission [17, 18]. Quasifission has been shown to hinder fusion (P_{CN} is reduced) by orders of magnitude [5, 19, 20] in some cases. A large effort has focused on understanding the entrance channel conditions that favor quasifission including: mass asymmetry [19], fissility of the compound nucleus [21, 22], reaction energy [17, 23], magicity [24, 25], and neutron-richess of the compound nucleus $(N/Z)_{CN}$ [25–32]. Heavy-ion fusion is further complicated by entrance channel nuclear structure effects including large static deformations in the heavy reaction partner [33–37].

The distribution of fission fragment mass with angle (the so called mass-angle distribution - MAD) has been used extensively to study quasifission reaction dynamics [18, 36–39]; in particular, Ref. [39] provides an overall view of MADs from reactions of medium mass projectiles and targets. Three regions were identified based on the shape of the quasifission mass distribution and the entrance channel charge product Z_pZ_t. The study of reactions at the intersection of two of these regions will provide important information on the quasifission mechanism. Cr + W is a prime candidate to study as its charge product, 1776, is at the intersection of reactions that show short time-scale quasifission (where the dinuclear system separates after very little rotation, with incomplete mass equilibrium leading to minimum yield at mass symmetry) and medium time-scale quasifission reactions (where the system rotates through larger angles and the fragments have time to move further towards mass equilibration, resulting in a peak in yield at mass-symmetry) [39].

Previous measurements of the Cr + W systems, at beam energies chosen to give a constant ratio to the respective interaction barriers V_B [40] showed that the compound nucleus $(N/Z)_{CN}$ was important in determining the characteristics including time scale of quasifission [32]. In the present work, the effect of changing the neutron-richness of the compound nucleus was explored for the same Cr + W systems, however at a constant excitation energy $E^* = 52.0$ MeV, closer to the interaction barrier than the reactions reported in [32] and similar to that used in hot-fusion reactions. This eliminates possible effects of variations in excitation energies in different reactions influencing the quasifission dynamics.

II. EXPERIMENTAL DETAILS

Beams of ^{50,52,54}Cr provided by the 14UD electrostatic accelerator and superconducting LINAC at the Heavy Ion Accelerator Facility at the Australian National University (ANU) were used to bombard isotopically enriched targets of ^{180,182,184,186}W with thicknesses ranging from $43-97$ μg/cm^2, mounted on $40-60$ μg/cm^2 carbon backings [42] which faced downstream. The details are given in Table I. Fragments resulting from fusion-fission and quasifission reactions (collectively termed fission-like) were detected in coincidence using the ANU CUBE detector system [43]. The detector system consisted of two large-area, position-sensitive multiwire proportional counters (MWPCs). A diagram of the CUBE detector set-up used in the present work is shown in Figure 1. Each MWPC had an active area of 28×36 cm^2 [39, 43] that were placed to cover laboratory scattering angles of $5^\circ < \theta < 80^\circ$ and $50^\circ < \theta < 125^\circ$. Time-of-flight and position information for coincident fission fragments allowed determination of their velocity vectors. The kinematic coincidence technique [18, 39, 44] was used in the analysis. It provided confirmation that the fission events resulted from full momentum transfer (full projectile capture) reactions, and allowed the mass ratio at scission $M_R = m_1/(m_1 + m_2)$ (where m_1 and m_2 are the masses of the fission fragments at scission) to be determined over all measured angles. Determination of the masses of the fission fragments detected would need information on pre-and post-scission particle emission, which was not measured, and is not required for the purposes of this work. Hence results are presented in terms of M_R.

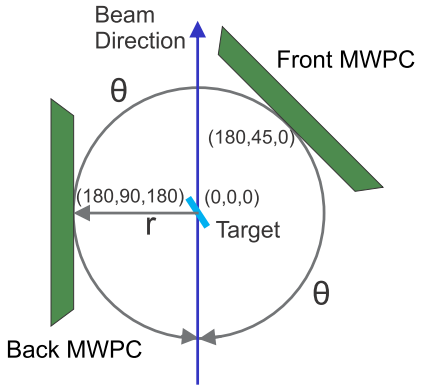

FIG. 1. Schematic scale diagram of the CUBE detector setup from above. The definitions of θ and r are indicated. The coordinates (r,θ,Φ) at the center of the CUBE and at the center of the two MWPCs are indicated, in mm and degrees.

From the list of the measured reactions given in Table I one can see that the most neutron-deficient (^{50}Cr $+^{180}$W) and neutron-rich (^{54}Cr $+^{186}$W) systems are different by ten neutrons, which provides an opportunity to study the $(N/Z)_{CN}$ dependence of the reactions while holding constant other variables that are known to affect the quasifission process. The Cr + W reactions all have the same entrance channel charge product Z_pZ_t of 1776, and only ^{52}Cr has a single closed shell at $N = 28$. The W targets are all prolate deformed, with calculated [45] β_2 values in the range 0.225 to 0.254, and β_4 values between -0.067 and -0.107 (^{186}W). The small variations in deformation parameters will not change the average capture barrier energies significantly, and since all of the

TABLE I. Projectile, target and compound nucleus, number of neutrons relative to the lightest compound nucleus ^{230}Cf corresponding to the ^{50}Cr + ^{180}W reaction, W target thickness, center of mass energy $E_{c.m.}$, excitation energy E^*_{CN}, $E_{c.m.}/V_B$, $(N/Z)_{CN}$, calculated l_{max} from the total reaction cross section [41], and l_{crit} [41] for each of the systems.

System	ΔN	Target Thickness (μg cm^{-1})	$E_{c.m.}$ (MeV)	E^*_{CN} (MeV)	$E_{c.m.}/V_B$	$(N/Z)_{CN}$	l_{max} ($\hbar$)	l_{crit} ($\hbar$)
^{50}Cr +^{180}W→^{230}Cf	0	48	210.0	52.0	1.07	1.35	67	58
^{50}Cr +^{186}W→^{236}Cf	6	43	201.3	52.0	1.03	1.41	44	39
^{52}Cr +^{180}W→^{232}Cf	2	48	214.1	52.0	1.09	1.37	76	71
^{52}Cr +^{184}W→^{236}Cf	6	64	209.7	52.0	1.08	1.41	72	64
^{54}Cr +^{180}W→^{234}Cf	4	46	215.4	52.3	1.11	1.39	85	76
^{54}Cr +^{182}W→^{236}Cf	6	97	213.8	52.0	1.10	1.41	81	75
^{54}Cr +^{184}W→^{238}Cf	8	64	211.8	52.0	1.09	1.43	76	72
^{54}Cr +^{186}W→^{240}Cf	10	43	209.5	52.0	1.08	1.45	72	69

measurements presented in this work are above-barrier, at the same excitation energy (E^* = 52.0 MeV), our results and conclusions will not be sensitive to these small variations.

III. RESULTS AND DISCUSSION

The effect of changing the neutron-richness on the reaction dynamics was explored by analyzing the mass-angle distributions (MAD) generated from the deduced mass ratios and center-of-mass angles ($\theta_{c.m.}$) [46]. The MADs for all eight of the Cr + W systems are shown in Figure 2. The MADs with M_R and $\theta_{c.m.}$ of the particle detected in the Back MWPC are shown in Panels a-d and i-l, whilst those corresponding to the Front MWPC are shown in Panels e-h and m-p. The corresponding distributions overlap, resulting in full coverage in the MAD over an angular range typically from 30° to 150° in the center-of-mass frame. The intense bands of events at $M_R \sim 0.2$ and 0.8 result from elastic, quasielastic and deep inelastic events with little mass drift away from the initial masses. The mass resolution for elastic scattering for these measurement is shown graphically in Figure 1 of Ref. [32]. This corresponds to an RMS deviation of 2.5 u for the elastic scattering events. The region between these two bands contains events from quasifission and fusion-fission, termed the fission-like region. In the present work, the fission-like region was defined to be between mass ratios of 0.35 and 0.65. The TKE distributions of these events are consistent with full energy damping for all reactions studied, consistent with previous quasifission measurements [18].

A notable feature in the fission-like region is the correlation between mass-ratio and angle. This correlation indicates that the reaction time (sticking time) is shorter than the rotation time. This is associated with the quasifission process. In contrast, fragments from fusion-fission reactions will be found at all angles and will form a narrower peak in the mass ratio distribution around $M_R = 0.5$ [18, 47]. A correlation between mass-ratio and angle was observed in each MAD in Figure 2, but no clear evidence of an angle-independent fusion-fission peak, indicating that the quasifission component is dominant.

The mass-ratio distributions (in counts), integrated over the full angular range covered by the detector system, for all eight of the Cr + W reactions are shown in Figure 3. The angular acceptance is essentially independent of mass-ratio (see Figure 2), so counts are proportional to cross section. The large peaks at $M_R \sim 0.2$ and 0.8 result mainly from elastic scattering events at forward angles. The very broad mass distributions in the fission-like region are also consistent with a prominent contribution from quasifission [18, 39].

Previously [25, 32, 35, 43, 44, 50–53] mass distributions were quantified and compared by fitting the fission-like region with a Gaussian function and extracting the Gaussian standard deviation. However, this method cannot be applied in the present work. This is clear from Figure 3, where two systems, ^{50}Cr+^{180}W (3 a) and ^{50}Cr+^{186}W (3 d), have a minimum yield at $M_R = 0.5$, and so cannot be characterized using a Gaussian function. Instead, each mass distribution was fitted in the fission-like region with a second degree polynomial function, symmetric about $M_R = 0.5$, using a chi-squared procedure. The resulting fitted functions all had reduced chi-squared values close to unity. The results of these fits are represented by the solid (pale blue) lines in each panel of Figure 3. The second derivative, determined as two times the second order coefficient of the function resulting from the fit, was used as a quantitative measure of the shape of the mass distributions, and is referred to as the curvature parameter. A more negative curvature parameter indicates that the mass distribution has a narrower peak in the fission-like region.

The curvature parameters determined for the mass distributions of the Cr + W systems are shown as a function of $(N/Z)_{CN}$ in Figure 4. While there is a general decrease in curvature with increasing neutron-richness the correlation is not as uniform as that previously reported for the

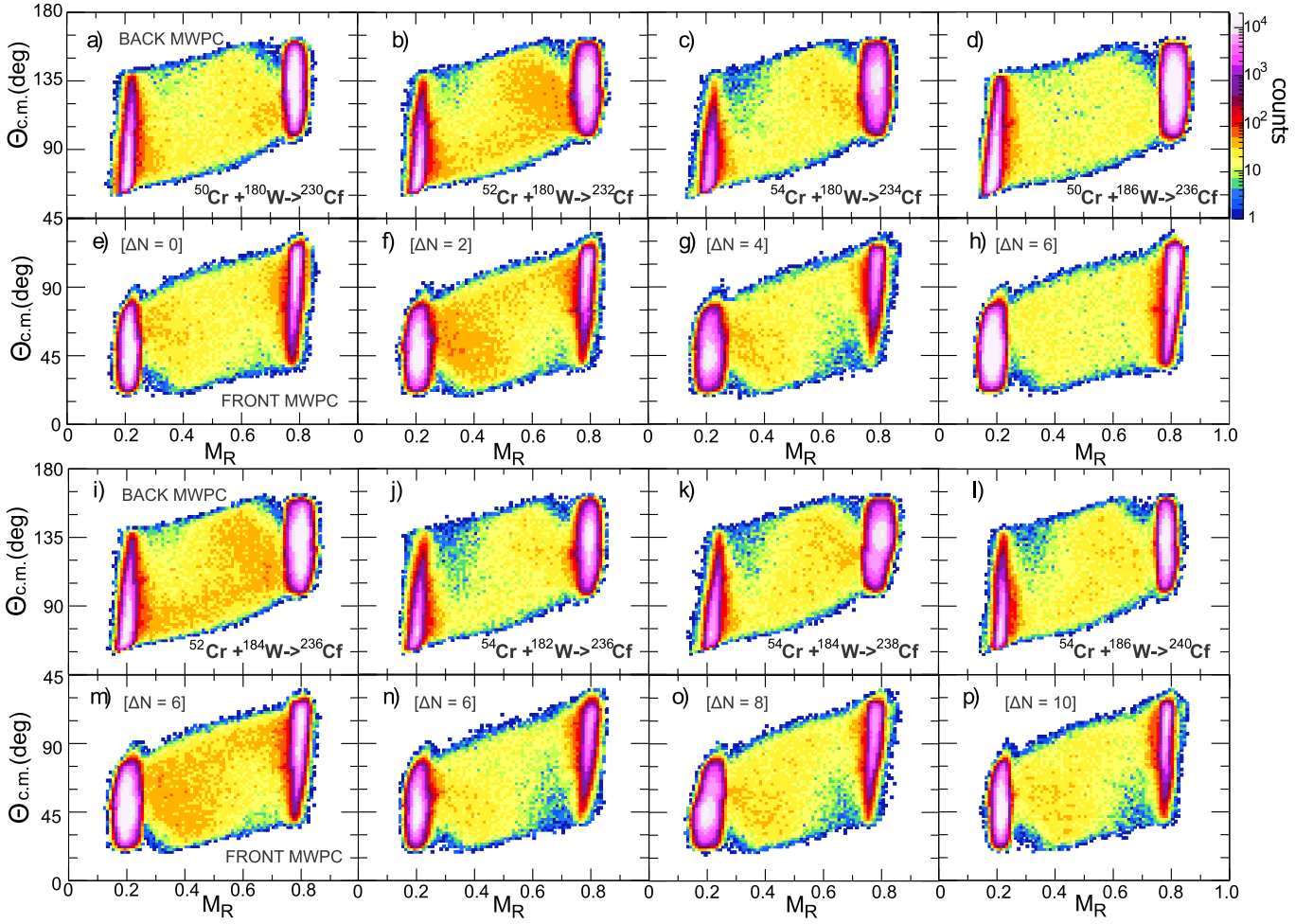

FIG. 2. (color online) The mass-angle distributions are shown for all eight Cr + W systems from the present work at $E^* = 52.0$ MeV. The color scale (top right) indicates the number of events per pixel, which is proportional to $d^2\sigma/d\theta dM_R$. In the first (Panels a-d) and third rows (Panels i-l) the MADs corresponding to the mass and angle of the fragment detected in the Back MWPC are shown. In the second (Panels e-h) and fourth (Panels m-p) rows the MADs corresponding to the Front MWPC are shown. For each system, the projectile, target, and number of neutrons relative to ^{230}Cf is given.

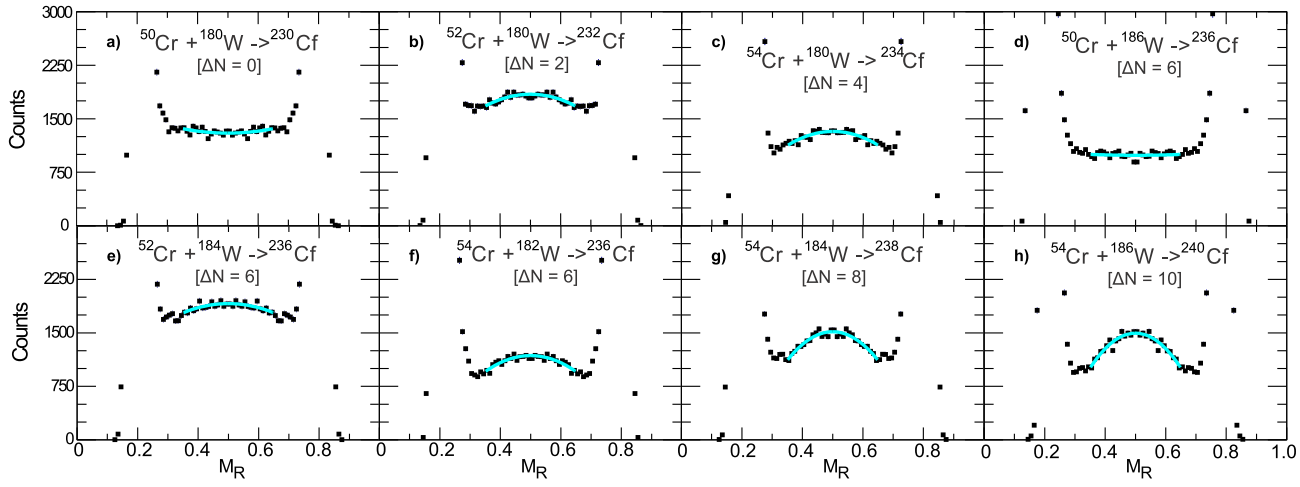

FIG. 3. (color online) The projected mass distributions are shown for all eight Cr + W systems from the present work at $E^* = 52.0$ MeV. The black points represent the experimental data. Experimental uncertainties are smaller than the size of the points. The full (blue) line shows a quadratic fit to the fission-like region. For each system, the projectile, target, compound nucleus, and number of neutrons relative to ^{230}Cf is given.

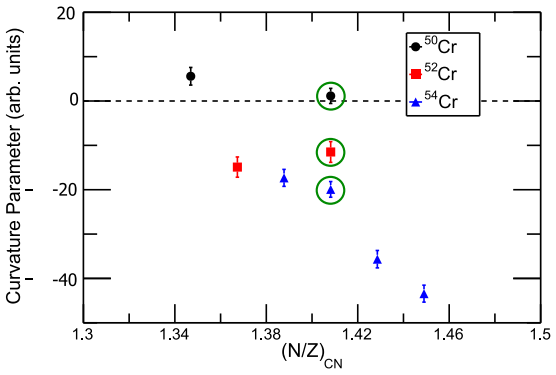

FIG. 4. The curvature parameters determined from the fit of the fission-like region of the mass distributions are shown as a function of $(N/Z)_{CN}$. The points corresponding to the reactions forming ^{236}Cf are highlighted by (green) circles.

Cr + W systems measured at a constant 13% above the Bass barrier [40] reported in [32]. The two systems discussed above having a positive curvature parameter are those where ^{50}Cr was the projectile. The weaker mass evolution towards symmetry suggests that the sticking time is shorter for these two measurements. It is likely that this is correlated with a lower probability of true fusion forming a compact compound nucleus.

A. Bohr Independence Hypothesis

The Bohr Independence Hypothesis [54] states that once a nucleus with a given angular momentum fully equilibrates in all degrees of freedom it loses all memory of the entrance channel. Thus, the decay of an equilibrated compound nucleus should be independent of the entrance channel through which it was produced.

The mass distributions of three systems where ^{236}Cf was the compound nucleus are shown in Panels d-f of Figure 3. As in the other reactions, for these systems the compound nucleus was formed at the same excitation energy of 52 MeV. If compound nucleus formation was the dominant reaction channel in these systems then the Bohr Independence Hypothesis should apply and the decay of these three systems should be the same, insofar as the angular momenta contributing are the same. Table I shows that for ^{52}Cr+^{184}W→^{236}Cf the calculated limiting angular momenta l_{crit} is slightly smaller than for ^{54}Cr+^{182}W→^{236}C, whilst ^{50}Cr+^{186}W→^{236}Cf has a much smaller l_{crit}. It is notable that the highest l_{crit} results in the narrowest mass distribution, and the smallest l_{crit} the widest. This difference between the systems can be observed in Figure 4 where the curvature parameters for all systems are shown as a function of $(N/Z)_{CN}$. The results for the three reactions forming ^{236}Cf all have $(N/Z)_{CN} = 1.41$, and are highlighted by (green) circles.

This observed dependence on l_{crit} is opposed to expectations for compound nucleus fission in this mass region [48]. In conjunction with the observed mass-angle correlations, these results confirm the presence of non-equilibrium processes. However, it is also opposite to expectations from non-equilibrium fission measurements reported in the literature which indicate that mass distributions generally become wider as angular momentum increases [17, 18, 49]. Thus the observation cannot be attributed *directly* to the effect of angular momentum itself on the dynamics. Other possible correlations are discussed below.

B. Fissility and Mass Asymmetry

The fissility of the compound nucleus χ_{CN} and the mass asymmetry of the entrance channel α are two parameters that change with the entrance channel, and are correlated with neutron-richness. χ_{CN} is inversely correlated with neutron-richness and defined as

$$\chi_{CN} = (Z^2/A)/(Z^2/A)_{crit} \quad (2)$$

where

$$(Z^2/A)_{crit} = 50.883(1 - 1.7826\ I^2) \quad (3)$$

and

$$I = (A - 2Z)/A \quad (4)$$

[21, 22]. Previous studies [21, 22] of the χ_{CN} dependence of quasifission observed a decrease in quasifission with decreasing χ_{CN}.

Mass asymmetry, defined as $\alpha = (A_{Target} - A_{Proj})/(A_{Target} + A_{Proj})$ also decreases as the neutron-richness of the projectile increases. Decreasing mass asymmetry, however, has been shown to lead to an increase in quasifission [17–19].

In many commonly used frameworks for interpretation of experimental data [21, 22, 30, 55–62] either the fissility or mass asymmetry is used as the dominant predictor of the importance of quasifission. Thus, the choice of model has resulted in conflicting conclusions as to the nature of the influence of neutron-richness on quasifission because of the differences between the correlation with fissility and the correlation with mass asymmetry. For example, measurements by Lesko *et al.* [27] and Liang *et al.* [29] of Sn + Ni systems showed that $(N/Z)_{CN}$ increased as the quasifission flux increased. However, measurements of Sn + Zr by Vinodkumar *et al.* [28] and Sahm *et al.* [26] found a decrease in quasifission as $(N/Z)_{CN}$ increased. Observations from previously reported measurements of Cr + W reactions at $E_{c.m.}/V_B = 1.13$ [32] indicated that as the neutron-richness changed, the character of the quasifission changed, but did not lead to a transition from dominantly quasifission to fusion-fission. In Figure 5, the curvature parameters determined for each system are shown as a function of χ_{CN} and α. The variation

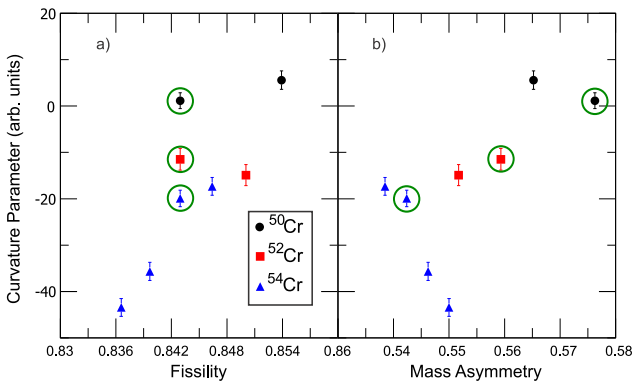

FIG. 5. The curvature parameter determined for each system as a function of compound nucleus fissility (χ_{CN}) (Panel a) and mass asymmetry (α) (Panel b). The points corresponding to the reactions forming ^{236}Cf are highlighted by (green) circles.

with α is opposite to general expectations of quasifission probability decreasing and sticking time increasing with increase in α (reduction in the mass of the projectile). There is considerable scatter of the curvature parameters when plotted against χ_{CN}, although there is a general increase in the curvature parameter with increasing fissility.

C. Rotational Energy

The center of mass energies for each system differed significantly to reach the same E^*_{CN} = 52.0 MeV. This resulted in large variations in the maximum rotational energy available to each system, calculated as $E_{rot} = E_{c.m.} - V_B$. The calculated maximum rotational energies carried by the systems measured in this work ranged from 5.75 to 20.56 MeV. While the systems with the lowest rotational energies have the highest curvature, there is not an overall correlation between maximum rotational energies and curvature, as seen in Figure 6. Note that the previously reported Cr + W systems [32], measured at $E_{c.m.}/V_B$ = 1.13, had a minimal change in rotational energy from 25.12 - 25.6 MeV, thus limiting the influence of this variable. In contrast, they showed a smoother change in quasifission outcome with $(N/Z)_{CN}$ than found in the measurements presented here. In Figure 4, the point with the largest deviation from a smooth dependence (black circle with surrounding green circle) is the point with the smallest rotational energy in Figure 6. This may give a clue to understand the experimental results, as discussed below.

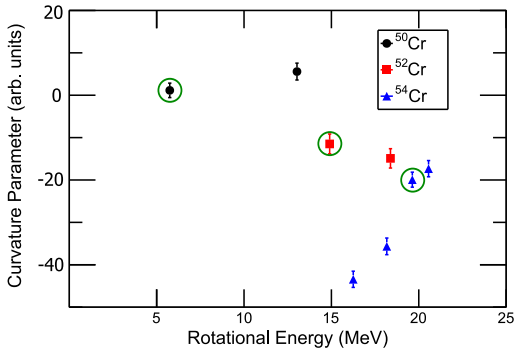

FIG. 6. (color online) The curvature parameter determined for each Cr + W system as a function of the maximum rotational energy E_{rot} (MeV). The points corresponding to the reactions forming ^{236}Cf are highlighted by (green) circles.

TABLE II. Bass average radii, β_2 values, semi-major radii, and semi-minor radii.

Nucleus	R(fm) (average)	β_2 [45]	R(fm) (semi-major)	R(fm) (semi-minor)
^{50}Cr	3.89	0.0	–	–
^{52}Cr	3.96	0.0	–	–
^{54}Cr	4.02	0.0	–	–
^{180}W	6.30	0.258	7.33	5.79
^{182}W	6.33	0.259	7.36	5.81
^{184}W	6.35	0.24	7.32	5.87
^{186}W	6.38	0.23	7.30	5.92

D. Deformation Effects

The ^{50,52,54}Cr nuclei can be approximated as spherical, but ^{180,182,184,186}W are all strongly deformed. The β_2 values calculated in [45] are shown in Table II. Accounting for the largest deformation parameter, which is β_2, the deformation of the W nuclei results in a $\sim$ 1 fm variation from the average radius of the semi-major and semi-minor radius, Table III.

To reach E^*_{CN} of 52.0 MeV, the center of mass energy for each reaction is lower and thus closer to the Bass barrier [40] relative to the energies necessary to reach $E_{c.m.}/V_B$ = 1.13. As shown by previous works [33, 36, 43, 44, 63–65], deformation has a large impact near the interaction barrier. In reactions of deformed nuclei, the barrier is dependent on the orientation of the deformed nucleus. Generally, the reported interaction barrier is an average of all possible collision orientations.

Many previous works [33, 34, 43, 44, 46, 66–68] have shown that at $E_{c.m.}$ near or below the interaction barrier the structure of the nuclei involved in a heavy-ion fusion reaction, particularly a heavy reaction partner with a large deformation, has a significant effect on the reac-

TABLE III. Barriers for average, aligned, and anti-aligned orientations for each measured reaction system.

System	V_{Bass}(MeV) (average)	V_{Bass}(MeV) (aligned)	V_{Bass}(MeV) (anti-aligned)
^{50}Cr +^{180}W	196.95	179.84	207.21
^{50}Cr +^{186}W	195.59	180.31	204.70
^{52}Cr +^{180}W	195.75	178.86	205.83
^{52}Cr +^{184}W	194.80	179.00	204.17
^{54}Cr +^{180}W	194.56	177.89	204.51
^{54}Cr +^{182}W	194.12	177.46	204.10
^{54}Cr +^{184}W	193.67	178.05	202.86
^{54}Cr +^{186}W	193.22	178.35	202.10

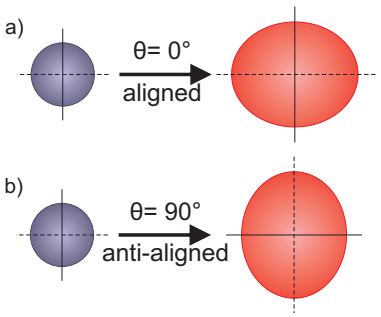

FIG. 7. Illustration of an aligned (Panel a) and an anti-aligned (Panel b) collision between a spherical projectile and a prolate target.

tion dynamics. When a deformed heavy nucleus takes part in the reaction the evaporation residue cross section was observed to be hindered at energies near and below the barrier [34, 68]. Similarly, at center-of-mass energies near the barrier, hindrance of the related fusion-fission reaction channel has also been attributed to the predominance of interactions with the deformation-aligned heavy nucleus in the entrance channel [33, 43, 44, 46, 66, 67], as detailed below. This loss in evaporation residue and fusion-fission production correlates with an increase in the strength of the quasifission reaction channel [33, 43].

It is useful to consider the change in the barrier for the two extreme collision types at an impact parameter b=0. When the nuclear deformation axis of the heavy prolate deformed nucleus is aligned with the approaching Cr, the collision is with the tip of the prolate W (Figure 7, Panel a). When the deformation axis is anti-aligned, the Cr interacts with the elongated side of the prolate W (Figure 7, Panel b).

Deformation-aligned collisions result in an elongated dinuclear system. This elongated shape leads to a preference for quasifission [33, 43, 44]. Conversely, anti-aligned collisions produce a compact dinuclear system that is likely to have a larger probability of forming a fully fused compact compound nucleus [33, 43, 44].

The interaction barriers were calculated for the two orientations described above. First, the deformed tungsten nucleus was approximated as an ellipsoid of revolution where the various radii can be calculated from the expression

$$R(\theta,\phi) = R_{\rm avg}[1 + \beta_2 \mathbf{Y}_{20}(\theta,\phi)] \quad (5)$$

where R_{avg} is the average radius of the two major axes, β_2 is the deformation parameter along the semi-major axis of interest, and $\mathbf{Y}_{20}$ is a spherical harmonic function ($\mathbf{Y}_{LM}$) where L is 2, M is 0, and β_4 is neglected [69]. In a prolate deformed nucleus, there are two axes of interest: (1) the elongated semi-major axis, along the nuclear symmetry axis which is indicated by the dashed, black line in the example prolate deformed nucleus in Figure 7, (2) the shortened semi-minor axis indicated by the solid, black line in the example prolate deformed nucleus in Figure 7. The limiting case of the semi-major and semi-minor axes can be calculated as:

$$R_{\rm semi-Major}(\theta,\phi) = R_{\rm avg}[1 - \frac{\beta_2}{4}\sqrt{\frac{5}{\pi}}] \quad (6)$$

$$R_{\rm semi-Minor}(\theta,\phi) = R_{\rm avg}[1 + \frac{\beta_2}{2}\sqrt{\frac{5}{\pi}}] \quad (7)$$

The radius used in the present work was taken to be the Blocki half-density radius [40] given by the expression $R_{avg} = 1.16 * A^{1/3} - 1.39 * A^{-1/3}$. The average, semi-major, and semi-minor radii are listed in Table II. The semi-major and semi-minor axes change by more than 1 fm compared to the average radius, or by about 10% of the total, because of the strong deformation of the W nuclei. This change in radius has a large effect on the interaction barrier associated with each case considered in this discussion. The interaction radius for a given orientation (θ as defined in Figure 7) was determined as $R_{int}(\theta) = R^{Cr}(\theta) + R^{W}(\theta)$. The Bass barriers [40] for all three orientations (averaged, aligned, and anti-aligned) are shown in Table III. As expected the barriers for the aligned collisions are lower than the average, while the barriers for the anti-aligned collisions are higher than the average barriers. In Figure 8, the curvature is plotted as a function of $E_{c.m.}$ / V_B for the average (Panel b), aligned (Panel a), and anti-aligned (Panel c) barriers with the dashed vertical line showing the barrier energy in each panel. For the two reactions of ^{50}Cr, the anti-aligned collision type is strongly hindered as $E_{c.m.}$ / $V_B(\text{anti} - \text{aligned}) = 0.98$ and 1.01.

Previous work [33, 34, 43, 44, 46, 66–68] has generally shown that, in reactions with heavy deformed nuclei, quasifission increases near and below the barrier. In the present case, fusion in the anti-aligned orientation will be hindered for the two ^{50}Cr reactions, therefore the majority of events that successfully capture and form a dinuclear system do so in the aligned (elongated) orientation which preferentially leads to rapid separation and

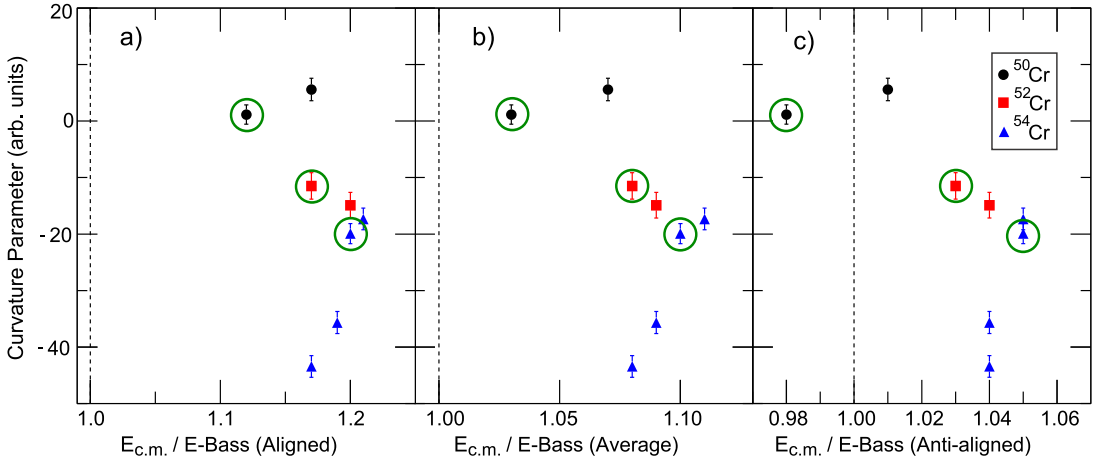

FIG. 8. (color online) The curvature parameter determined for each system as a function of $E_{c.m.}$ / V_B for all Cr + W system where V_B is taken as the aligned barrier (Panel a), the average barrier (Panel b), and the anti-aligned barrier (Panel c). The dashed line denotes the barrier in each panel. The points corresponding to the reactions forming ^{236}Cf are highlighted by (green) circles.

quasifission. The other systems in this work are able to capture in all orientations, including those that favour longer sticking times and fusion-fission, resulting in a lowered curvature of the observed mass distributions.

IV. CONCLUSIONS

Fission fragment mass distributions were measured for a series of Cr + W reactions at the same compound nucleus excitation energy $E^*_{CN} = 52$ MeV. A curvature parameter was defined to characterize each mass distribution, a positive value corresponding to a minimum at mass-symmetry, and more negative values corresponding to an increasingly prominent peak at mass-symmetry. The latter is consistent with a longer sticking time, allowing more mass evolution towards the energetically favoured mass-symmetric split. The Bohr Independence Hypothesis was not followed for three systems that form the same compound nucleus ^{236}Cf. Unlike the previously Cr + W measurements at the same energy above the respective capture barriers, namely $E_{c.m.}$ / V_B = 1.13, there was more scatter between the curvature of the mass distribution and $(N/Z)_{CN}$. Plotting the curvature parameter as a function of compound nuclear fissility, mass asymmetry, or rotational energy does not eliminate the scatter - for the latter two, it increases. However, the significant anti-correlation of curvature with rotational energy for the three reactions forming ^{236}Cf gives an indication as to why the quasifission characteristics show more scatter than the previous results for the same Cr + W systems measured at $E_{c.m.}$ / V_B = 1.13. The reactions with ^{50}Cr, with minimum fission yield at symmetry, were measured at the lowest $E_{c.m.}$ / V_B to achieve the same 52 MeV excitation energy. At beam energies close to the mean capture barrier, the strong shift of the fusion barrier energy depending on the orientation of the deformed W target nuclei significantly hinders the more compact dinuclear orientations that favor long sticking times (and presumably fusion). It is proposed that this leads to shorter sticking times, and a minimum in mass-yield at mass-symmetry for the ^{50}Cr +^{180}W and ^{50}Cr +^{186}W measurements reported here.

The present work demonstrates that at energies near the interaction barrier, target deformation effects are as important as neutron-richness in determining the quasifission characteristics in these Cr + W reactions, and both are important considerations in choosing reactions to form new heavy and superheavy element and isotopes.

Acknowledgments. The authors are grateful for the high quality beams provided by the staff at the ANU accelerator facility. This work is supported by the National Science Foundation under Grants No. PHY-1102511 and No. IIA-1341088, by the U.S. Department of Energy under Grant No. DE-FG02-96ER40975 with Vanderbilt University, and the Australian Research Council Grants DP160101254, DP170102318, DP140101337, FL110100098, DP130101569, FT120100760, and DE140100784. This material is based upon work supported by the Department of Energy National Nuclear Security Administration through the Nuclear Science and Security Consortium under Award Number DE-NA0000979.

[1] Yu. Ts. Oganessian, V. K. Utyonkov, Yu. V. Lobanov, F. Sh. Abdullin, A. N. Polyakov, R. N. Sagaidak, I. V. Shirokovsky, Yu. S. Tsyganov, A. A. Voinov, G. G. Gul-

bekian, S. L. Bogomolov, B. N. Gikal, A. N. Mezentsev, S. Iliev, V. G. Subbotin, A. M. Sukhov, K. Subotic, V. I. Zagrebaev, G. K. Vostokin, M. G. Itkis, K. J. Moody, J. B. Patin, D. A. Shaughnessy, M. A. Stoyer, N. J. Stoyer, P. A. Wilk, J. M. Kenneally, J. H. Landrum, J. F. Wild, and R. W. Lougheed, Phys. Rev. C **74** 044602 (2006).

[2] Yu. Ts. Oganessian, F. S. Abdullin, C. Alexander, J. Binder, R. A. Boll, S. N. Dmitriev, J. Ezold, K. Felker, J. M. Gostic, R. K. Grzywacz, J. H. Hamilton, R. A. Henderson, M. G. Itkis, K. Miernik, D. Miller, K. J. Moody, A. N. Polyakov, A. V. Ramayya, J. B. Roberto, M. A. Ryabinin, K. P. Rykaczewski, R. N. Sagaidak, D. A. Shaughnessy, I. V. Shirokovsky, M. V. Shumeiko, M. A. Stoyer, N. J. Stoyer, V. G. Subbotin, A. M. Sukhov, Y. S. Tsyganov, V. K. Utyonkov, A. A. Voinov, and G. K. Vostokin, Phys. Rev. Lett. **109**, 162501 (2012).

[3] Yu. Ts. Oganessian, and V. K. Utyonkov, Rep. Prog. Phys. **78**, 36301 (2015).

[4] Y. Oganessian, J. Phys. G **34**, R165 (2007).

[5] J. Hamilton, S. Hofmann, and Y. Oganessian, Ann. Rev. Nucl. Part. S. **63**, 383 (2013).

[6] S. Hofmann, S. Heinz, R. Mann, J. Maurer, G. Munzenberg, S. Antalic, W. Barth, H. G. Burkhard, L. Dahl, K. Eberhardt, R. Grzywacz, J. H. Hamilton, R. A. Henderson, J. M. Kenneally, B. Kindler, I. Kojouharov, R. Lang, B. Lommel, K. Miernik, D. Miller, K. J. Moody, K. Morita, K. Nishio, A. G. Popeko, J. B. Roberto, J. Runke, K. P. Rykaczewski, S. Saro, C. Scheidenberger, H. J. Schott, D. A. Shaughnessy, M. A. Stoyer, P. Thorle-Pospiech, K. Tinschert, N. Trautmann, J. Uusitalo, and A. V. Yeremin, Eur. Phys. J. A **52**, 180 (2016).

[7] S. Hofmann and G. Munzenberg, Rev. Mod. Phys. **72**, 733 (2000).

[8] M. Bender, K. Rutz, P.-G. Reinhard, J. A. Maruhn, and W. Greiner, Phys. Rev. C **60** 034304(1999).

[9] Y. T. Oganessian, F. S. Abdullin, P. D. Bailey, D. E. Benker, M. E. Bennett, S. N. Dmitriev, J. G. Ezold, J. H. Hamilton, R. A. Henderson, M. G. Itkis, Y. V. Lobanov, A. N. Mezentsev, K. J. Moody, S. L. Nelson, A. N. Polyakov, C. E. Porter, A. V. Ramayya, F. D. Riley, J. B. Roberto, M. A. Ryabinin, K. P. Rykaczewski, R. N. Sagaidak, D. A. Shaughnessy, I. V. Shirokovsky, M. A. Stoyer, V. G. Subbotin, R. Sudowe, A. M. Sukhov, Y. S. Tsyganov, V. K. Utyonkov, A. A. Voinov, G. K. Vostokin, and P. A. Wilk, Phys. Rev. Lett. **104**, 142502 (2010).

[10] M. Bender, W. Nazarewicz, and P.-G. Reinhard, Phys. Lett. B **515**, 42 (2001).

[11] W. Nazarewicz, M. Bender, S. Cwiok, P. H. Heenen, A. T. Kruppa, P.-G. Reinhard, and T. Vertse, Nucl. Phys. **A701**, 165 (2002).

[12] S. Hofmann, Prog. Part. Nucl. Phys. **46**, 293 (2001).

[13] S. Hofmann, J. Phys. G: Nucl. Part. Phys. **42**, 114001 (2015).

[14] W. Loveland, Phys. Rev. C **76**, 014612 (2007).

[15] R. Smolanczuk, Phys. Rev. C **81**, 067602 (2010).

[16] D. J. Hinde, M. Dasgupta, and A. Mukherjee, Phys. Rev. Lett. **89**, 282701 (2002).

[17] B. B. Back, Phys. Rev. C **31**, 2104 (1985).

[18] J. Tōke, R. Bock, G. X. Dai, A. Gobbi, S. Gralla, K. D. Hildenbrand, J. Kuzminski, W. F. J. Müller, A. Olmi, and H. Stelzer, Nucl. Phys. **A440**, 327 (1985).

[19] A. C. Berriman, D. J. Hinde, M. Dasgupta, C. R. Morton, R. D. Butt, and J. O. Newton, Nature **413**, 144 (2001).

[20] R. Yanez, W. Loveland, J. S. Barrett, L. Yao, B. B. Back, S. Zhu, and T. L. Khoo, Phys. Rev. C **88**, 014606 (2013).

[21] W. J. Swiatecki, Nucl. Phys. **A376**, 275 (1982).

[22] S. Bjørnholm and W. J. Swiatecki, Nucl. Phys. **A391**, 471 (1982).

[23] M. B. Tsang, H. Utsunomiya, C. K. Gelbke, W. G. Lynch, B. B. Back, S. Saini, P. A. Baisden, and M. A. McMahan, Phys. Lett. **129**, 18 (1983).

[24] M. Itkis, A. A. Bogachev, I. Itkis, J. Kliman, G. Knyazheva, N. Kondratiev, E. Kozulin, L. Krupa, Y. Oganessian, I. Pokrovsky, E. Prokhorova, and A. Rusanov, Nucl. Phys. **A787**, 150 (2007).

[25] C. Simenel, D. J. Hinde, R. du Rietz, M. Dasgupta, M. Evers, C. Lin, D. Luong, and A. Wakhle, Phys. Lett. B **710**, 607 (2012).

[26] C. C. Sahm, H. G. Clerc, K. H. Schmidt, W. Reisdorf, P. Armbruster, F. P. Hessberger, J. G. Keller, G. Munzenberg, and D. Vermeulen, Nucl. Phys. **A441**, 316 (1985).

[27] K. T. Lesko, W. Henning, K. E. Rehm, G. Rosner, J. P. Schiffer, G. S. F. Stephans, B. Zeidman, and W. S. Freeman, Phys. Rev. C **34**, 2155 (1986).

[28] A. M. Vinodkumar, W. Loveland, J. J. Neeway, L. Prisbrey, P. H. Sprunger, D. Peterson, J. F. Liang, D. Shapira, C. J. Gross, R. L. Varner, J. J. Kolata, A. Roberts, and A. L. Caraley, Phys. Rev. C **78**, 054608 (2008).

[29] J. F. Liang, C. J. Gross, Z. Kohley, D. Shapira, R. L. Varner, J. M. Allmond, A. L. Caraley, K. Lagergren, and P. E. Mueller, Phys. Rev. C **85**, 031601(R) (2012).

[30] G. Adamian, N. Antonenko, and W. Scheid, Nucl. Phys. **A678**, 24 (2000).

[31] C. Wang, J. Zhang, Z. Z. Ren, and C. W. Shen, Phys. Rev. C **82**, 054605 (2010).

[32] K. Hammerton, Z. Kohley, D. J. Hinde, M. Dasgupta, A. Wakhle, E. Williams, V. E. Oberacker, A. S. Umar, I. P. Carter, K. J. Cook, J. Greene, D. Y. Jeung, D. H. Luong, S. D. McNeil, C. S. Palshetkar, D. C. Rafferty, C. Simenel, and K. Stiefel, Phys. Rev. C **91**, 041602(R) (2015).

[33] D. J. Hinde, M. Dasgupta, J. R. Leigh, J. P. Lestone, J. C. Mein, C. R. Morton, J. O. Newton, and H. Timmers, Phys. Rev. Lett. **74**, 1295 (1995).

[34] K. Nishio, H. Ikezoe, S. Mitsuoka, K. Satou, and S. C. Jeong, Phys. Rev. C **63**, 044610 (2001).

[35] C. J. Lin, R. du Rietz, D. J. Hinde, M. Dasgupta, R. G. Thomas, M. L. Brown, M. Evers, L. R. Gasques, and M. D. Rodriguez, Phys. Rev. C **85**, 014611 (2012).

[36] A. Wakhle, C. Simenel, D. J. Hinde, M. Dasgupta, M. Evers, D. H. Luong, R. du Rietz, and E. Williams, Phys. Rev. Lett. **113**, 182502 (2014).

[37] C. Simenel, in *Clusters in Nuclei, Volume 3*, Lecture Notes in Physics, Vol. 875, edited by C. Beck (Springer International Publishing, 2014) pp. 95–145.

[38] D. J. Hinde, R. G. Thomas, R. du Rietz, A. Diaz-Torres, M. Dasgupta, M. L. Brown, M. Evers, L. R. Gasques, R. Rafiei, and M. D. Rodriguez, Phys. Rev. Lett. **100**, 202701 (2008).

[39] R. du Rietz, E. Williams, D. J. Hinde, M. Dasgupta, M. Evers, C. J. Lin, D. H. Luong, C. Simenel, and A. Wakhle, Phys. Rev. C **88**, 054618 (2013).

[40] R. Bass, Phys. Rev. Lett. **39**, 265 (1977).

[41] O. B. Tarasov and D. Bazin, Nuclear Inst. and Methods

in Physics Research, B **204**, 174 (2003).
[42] J. P. Greene and Z. Kohley, J Radioanal Nucl Chem **305**, 743 (2015).
[43] D. J. Hinde, M. Dasgupta, J. R. Leigh, J. C. Mein, C. R. Morton, J. O. Newton, and H. Timmers, Phys. Rev. C **53**, 1290 (1996).
[44] D. J. Hinde, R. du Rietz, M. Dasgupta, R. G. Thomas, and L. R. Gasques, Phys. Rev. Lett. **101**, 092701 (2008).
[45] P. Möller, J. R. Nix, W. D. Myers, and W. J. Swiatecki, Atomic Data and Nuclear Data Tables **59**, 185 (1995).
[46] R. G. Thomas, D. J. Hinde, D. Duniec, F. Zenke, M. Dasgupta, M. L. Brown, M. Evers, L. R. Gasques, M. D. Rodriguez, and A. Diaz-Torres, Phys. Rev. C **77**, 034610 (2008).
[47] L. J. Colby Jr., M. L. Shoap, and J. W. Cobble, Physical Review **121**, 1451 (1961).
[48] E. G. Ryakov, A. V. Karpov, and G. D. Adeev, Physics of Particles and Nuclei Letters **4**, 29 (2007).
[49] C. Lebrun, F. Hanappe, J. F. Lecolley, F. Lefebvres, C. Ngô, J. Péter, and B. Tamain, Nucl. Phys. **A321**, 207 (1979).
[50] E. Prokhorova, A. A. Bogachev, M. Itkis, I. Itkis, G. Knyazheva, N. Kondratiev, E. Kozulin, L. Krupa, Y. Oganessian, I. Pokrovsky, V. Pashkevich, and A. Rusanov, Nucl. Phys. **A802**, 45 (2008).
[51] E. Williams, D. J. Hinde, M. Dasgupta, R. du Rietz, I. P. Carter, M. Evers, D. H. Luong, S. D. McNeil, D. C. Rafferty, K. Ramachandran, and A. Wakhle, Phys. Rev. C **88**, 034611 (2013).
[52] I. M. Itkis, E. M. Kozulin, M. G. Itkis, G. N. Knyazheva, A. A. Bogachev, E. V. Chernysheva, L. Krupa, Y. T. Oganessian, V. I. Zagrebaev, A. Y. Rusanov, F. Goennenwein, O. Dorvaux, L. Stuttgé, F. Hanappe, E. Vardaci, and E. de Goés Brennand, Phys. Rev. C **83**, 064613 (2011).
[53] M. G. Itkis, J. Aystob, S. Beghini, A. A. Bogache, L. Corradid, M. G. Itkis, J. Aystob, S. Beghini, A. A. Bogachev, L. Corradi, O. Dorvaux, A. Gadea, G. Giardina, F. Hanappe, I. M. Itkis, M. Jandel, J. Kliman, S. V. Khlebnikov, G. N. Kniajeva, N. A. Kondratiev, E. M. Kozulin, L. Krupa, A. Latina, T. Materna, G. Montagnoli, Y. T. Oganessian, I. V. Pokrovsky, E. V. Prokhorova, N. Rowley, V. A. Rubchenya, A. Y. Rusanov, R. N. Sagaidak, F. Scarlassara, A. M. Stefanini, L. Stuttge, S. Szilner, M. Trotta, W. H. Trzaska, D. N. Vakhtin, A. M. Vinodkumar, V. M. Voskressenski, and V. I. Zagrebaev, Nucl. Phys. **A734**, 136 (2004).
[54] N. Bohr, Nature **137**, 344 (1936).
[55] V. I. Zagrebaev, Y. Aritomo, M. G. Itkis, Y. T. Oganessian, and M. Ohta, Phys. Rev. C **65**, 014607 (2001).
[56] V. Zagrebaev, and W. Greiner, in *Clusters in Nuclei, Volume 1*, Lecture Notes in Physics, Vol. 818, edited by C. Beck (Springer International Publishing, 2010) pp. 267–315.
[57] B.B. Back, H. Esbensen, C.L. Jiang, and K.E. Rehm, Rev. Mod. Phys. **86**, 317 (2014).
[58] G. Adamian, N. Antonenko, and W. Scheid, in *Clusters in Nuclei, Volume 2*, Lecture Notes in Physics, Vol. 848, edited by C. Beck (Springer International Publishing, 2012) pp. 165–227.
[59] N. Antonenko, E. Cherepanov, A.K. Nasirov, V. Permjakov, and V. Volkov, Phys. Lett. B **319**, 425 (1993).
[60] N. V. Antonenko, E. A. Cherepanov, A. K. Nasirov, V. P. Permjakov, and V. V. Volkov, Phys. Rev. C **51**, 2635 (1995).
[61] J. P. Blocki, H. Feldmeier, and W. J. Swiatecki, Nucl. Phys. **A459**, 145 (1986).
[62] G. G. Adamian, N. V. Antonenko, and W. Scheid, Phys. Rev. C **68**, 034601 (2003).
[63] K. Nishio, S. Hofmann, F. P. Heßberger, D. Ackermann, S. Antalic, Y. Aritomo, V. F. Comas, C. E. Düllmann, A. Gorshkov, R. Graeger, K. Hagino, S. Heinz, J. A. Heredia, K. Hirose, H. Ikezoe, J. Khuyagbaatar, B. Kindler, I. Kojouharov, B. Lommel, R. Mann, S. Mitsuoka, Y. Nagame, I. Nishinaka, T. Ohtsuki, A. G. Popeko, S. Saro, M. Schädel, A. Türler, Y. Watanabe, A. Yakushev, and A. V. Yeremin, Phys. Rev. C **82**, 024611 (2010).
[64] G. N. Knyazheva, E. M. Kozulin, R. N. Sagaidak, A. Y. Chizhov, M. G. Itkis, N. A. Kondratiev, V. M. Voskressensky, A. M. Stefanini, B. R. Behera, L. Corradi, E. Fioretto, A. Gadea, A. Latina, S. Szilner, M. Trotta, S. Beghini, G. Montagnoli, F. Scarlassara, F. Haas, N. Rowley, P. R. S. Gomes, and A. Szantode Toledo, Phys. Rev. C **75**, 064602 (2007).
[65] K. Nishio, H. Ikezoe, S. Mitsuoka, I. Nishinaka, Y. Nagame, Y. Watanabe, T. Ohtsuki, K. Hirose, and S. Hofmann, Phys. Rev. C **77**, 064607 (2008).
[66] D. J. Hinde, M. Dasgupta, B. R. Fulton, C. R. Morton, R. J. Wooliscroft, A. C. Berriman, and K. Hagino, Phys. Rev. Lett. **89**, 272701 (2002).
[67] R. Rafiei, R. G. Thomas, D. J. Hinde, M. Dasgupta, C. R. Morton, L. R. Gasques, M. L. Brown, and M. D. Rodriguez, Phys. Rev. C **77**, 024606 (2008).
[68] S. Mitsuoka, H. Ikezoe, K. Nishio, K. Satou, and J. Lu, Phys. Rev. C **65**, 054608 (2002).
[69] W. Loveland, D. Peterson, A. M. Vinodkumar, P. H. Sprunger, D. Shapira, J. F. Liang, G. A. Souliotis, D. J. Morrissey, and P. Lofy, Phys. Rev. C **74**, 044607 (2006).